SITE EFFECT AND Q-FACTOR ESTIMATION OF ARASBARAN (AHAR-VARZAGHAN) EARTHQUAKE, IRAN BY SPECTRAL INVERSION METHOD

Sepehr RAJABI BANIANI* Supervisor: Toshiaki YOKOI**
MEE12605

ABSTRACT

This study is done in order to obtain site effect and attenuation regarding the Arasbaran (Ahar-Varzaghan) Earthquake on August 11th, 2012 in Iran. The region has one of the highest levels of seismic hazard. However, there are no advanced studies in this area in order to obtain site effect and *Q-factor*. Thus, the main aim of this study is to figure out the site effect and amplification by using the spectral inversion method with respect to geological parameters on the region. We selected 35 events and 13 stations to estimate the site effect and *Q-factor*. ω^{-2} model was used to estimate source parameters such as the corner frequency (f_0) and the seismic moment (M_0). Eventually, we obtained $Q = 45.85\, f^{1.495}$. Furthermore, the result shows high amplifications in Meshgin Shahr, Horand, Damirchi, Chaykandi, Khajeh and Kharvanagh. Although the reference site is not necessary, the usage of the reference events, especially the determination of the source parameters, can be quiet tough. It may be better to use a rock site or to conduct the geophysical exploration in sites where not so deep sediment is expected.

Keywords: Arasbaran (Ahar-Varzaghan) earthquake, site effect, *Q*-value, ω^{-2} model

1. INTRODUCTION

Iran is on the plate located between the Arabian plate and Eurasia plate. Due to this situation, the country has high seismic hazard. Almost all parts of the country are covered by major faults and high hazard areas. On August 11th , 2012 the Arasbaran (Ahar-Varzaghan) twin earthquakes occurred near Varzaghan and Ahar in Eastern Azerbaijan Province of the Northwest of Iran at 16:53 and 17:04 (local time) with magnitude 6.2 (IGUT) and 6.0 (IGUT) respectively with the depth around 12 km (The Institute of Geophysics, University of Tehran). For the quantitative estimation of strong ground motions, the site, path and the source effects are essential and these parameters are indispensable for predicting seismic ground motions. Thus, the main aim of the present paper is to determine the site effect and *Q* value using accelerograms of the Arasbaran twin earthquakes and their aftershocks based on the ω^{-2} model of seismic source.

2. ANALYSIS

The method which was used in this study is categorized as spectral inversion method that was first proposed by Andrews (1986), of which the biggest advantage is that the method can separate the source, path and site terms (Iwata and Irikura, 1988). The observed spectra of an earthquake in the frequency domain can be written as the product of the source, path, and site effects as,

$$O_{ij}(f) = S_i(f)G_j(f)R_{ij}^{-1}e^{-\pi f R_{ij}/Q(f)\beta}, \quad (1)$$

*Geological Survey of Iran.

**Director, International Institute of Seismology and Earthquake Engineering, BRI, Japan.

where $O_{ij}(f)$ denotes the observed spectra of the i-th earthquake at the j-th station, $S_i(f)$ the source of the i-th earthquake, $G_j(f)$ the site effect at the j-th station, R_{ij} the hypocentral distance from the i-th event to the j-th station, β the shear wave velocity, and $Q(f)$ the frequency dependent quality factor (Iwata and Irikura, 1988). From Eq. (1), the observed amplitude spectral ratio for the i-th event between divisor site $O_{ir}(f)$ and other stations $O_{ij}(f)$ is,

$$\frac{O_{ij}(f)}{O_{ir}(f)} = \frac{G_j(f)R_{ij}^{-1}e^{-\pi f R_{ij}/Q(f)\beta}}{G_j(f)R_{ir}^{-1}e^{-\pi f R_{ij}/Q(f)\beta}}, \quad (2)$$

where subscript r indicates the divisor site. Taking logarithm of Eq. (2) gives,

$$\ln[G_j(f)] - \ln[G_r(f)] - \pi f(R_{ij}-R_{ir})/Q(f)\beta = \ln[O_{ir}^{ij}(f)R_{ir}^{ij}], \quad (3)$$

where $O_{ir}^{ij}(f)$ is the ratio of the observed spectra of the i-th event at the j-th site with respect to the divisor site and R_{ir}^{ij} is hypocentral distance ratio between i-th event at j-th station with regard to the divisor site. If there are earthquakes of which seismic moment and corner frequency are known, the following constraint equation is available.

$$\ln[G_j(f)] - \pi f R_{ij}/Q(f)\beta = \ln[O_{ij}(f)R_{ij}] - \ln[S_i(f)] \quad (4)$$

Then matrix for inversion is taken from Eqs. (3) and (4):

$$\begin{bmatrix} A \\ c \end{bmatrix}[x] = \begin{bmatrix} b \\ d \end{bmatrix} \quad (5)$$

A corresponds to the left member of Eq. (3) and c is the left member of Eq. (4) , x is the unknown parameters that are site effects $G_j(f)$ and $Q^{-1}(f)$, and b and d are right members of Eq. (3) and Eq. (4), respectively. This study differs from Moya and Irikura (2003); they use the observed displacement spectra for $O_{ij}(f)$, whereas in this study the observed acceleration spectra is used. Thus the Eq. (6) written as following,

$$S_i(f) = a_{oi}/\{1+(f_{oi}/f)^2\}, \quad (6)$$

where $a_{oi}=(2\pi f_{oi})2\Omega_{oi}$ denotes the high frequency asymptote of the acceleration spectra, i.e., the acceleration flat level, $\Omega_{oi}=0.55M_{oi}/4\pi\rho\beta^3$, ρ=2,700 kg/m^3, β=3.0 Km/s. Here, the radiation coefficient averaged over azimuth and take-off angle on the logarithmic axis, 0.55 is used (Boore and Boatwright, 1984).

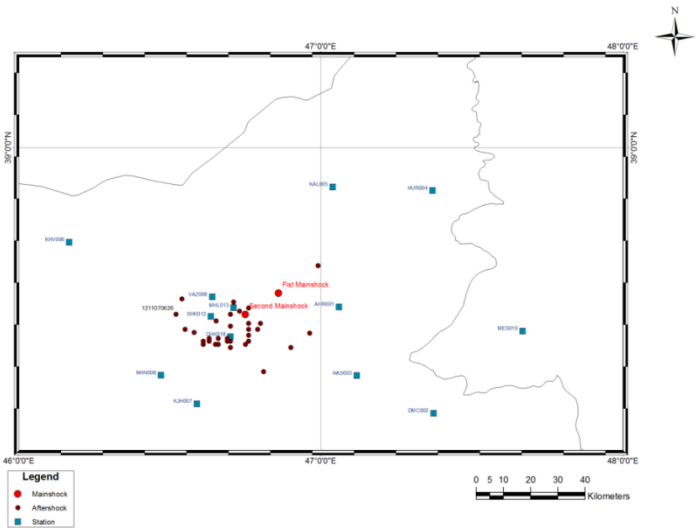

Figure 1. Epicenters and stations used for analysis.

In this study mainly the digital accelerograms provided by the strong motion observation network of the Building and Housing Research Center (BHRC), Iran were used. The digital seismograms of broadband stations of the Iranian National Broadband Seismic Network belongs to International Institute of Engineering Earthquake and Seismology (INSN-IIEES) were used also for the estimation of the corner frequency of the reference events.

Moreover, 138 records of 33 aftershocks were obtained at 13 stations (Figure 1).

2.1. Fourier Spectral Analysis of the First Mainshock

The first mainshock was selected as the reference event and its corner frequency was estimated using the digital seismogram of Maku station of INSN. First, the data of Maku station are analyzed by Fast Fourier Transform (FFT) using the time window of 63 to 127 seconds from S-wave on set. Corner frequency was determined around 0.178 Hz for the first mainshocks using the flat level of the displacement spectra Ω_0 and that of the acceleration spectra a_0 and from Eq. (7) the corner frequency was estimated. However, the reading value can have uncertainty and affect the result of analysis.

$$f_0 = \frac{1}{2\pi}\sqrt{\frac{a_0}{\Omega_0}} = 0.178\ Hz \tag{7}$$

2.2. Pre-Processing of the Strong Motion Records

In this study, the three-component waveforms recorded at 57, 75, 18 stations of the Iranian strong-motion network of BHRC during the first, second mainshocks and 33 aftershocks, respectively were downloaded. According to the BHRC the magnitude for the first mainshock was 6.2 and the second mainshock was 6.0. On the other hand, IRSC determined 6.5 and 6.3 for the first and the second mainshock, whereas USGS gave 6.4 for the first one. 35 events were chosen and 257 waveforms were analyzed including mainshocks and aftershocks started from August 11th, 2012 12:23:18 UTC to November 7th, 2012 06:26:31UTC and ranged magnitude from 3.7 to 6.2 with local depth less than 20 km. In order to obtain the Fourier spectra of S-waves which is the strongest part of the shaking, Husid plot was used (Husid, 1967). The window which was used for this calculation was 0.05 and 0.95 times to the total energy. In this part, the Husid plot is obtained from S-wave and it is indispensable to check the S-wave arrival time. Where the Husid plot *H(t)* is defined as follow,

$$H(t) = \frac{\int_0^t [a(t)]^2 dt}{\int_0^\infty [a(t)]^2 dt} \tag{8}$$

where *a(t)* is acceleration time history. In this study, the S-wave arrival was determined using *H(t)*=0.05, whereas the duration of the time window for Fast Fourier Transform is fixed at 10 seconds.

2.3. Fourier Spectral Analysis of the Strong Motion Records

Waveforms were analyzed to calculate amplitude and displacement spectra to make sure that the data quality is acceptable for the 35 events at the 75 stations, in total 170 spectra, by FFT. The increasing amplitude at the frequency band lower than 0.4 Hz was emphasized in the displacement amplitude spectra this is due to the low frequency noise included in accelerograms which may disturb the analysis.

2.4. Spectral Ratio Analysis for another Reference Event.

The frequency range of analysis was chosen from 0.2 Hz to 10 Hz, and then the records of which peak ground acceleration (PGA) is between 10 and 200 cm/s^2 were selected in order to exclude the records that may include the effect of non-linearity and also those of insufficient Signal to Noise ratio. Varzaghan (VAZ009), Horand (HUR004) and Mehtarloo (MHL013) were selected as the divisor sites. The first mainshock was selected for a reference event, whereas the second mainshock was not used due to the possibility of a complex rupture process. The event 1211070626 was selected as the second reference event to cover the second group of the records. From Eq. (1), the ratio of the observed spectra corrected using the hypocentral distance is formulated as follows.

$$F(f)= O_{is}\, R_{is} / O_{il}\, R_{il} = \Omega_{ol}^{os} \times (\{1 + (f/f_{ol})^2\}/\{1 + (f/f_{os})^2\}) \quad (9)$$

where Ω_{ol}^{os} is the ratio of the low frequency flat level of the smaller event to the bigger event, f_{os} is the corner frequency of the smaller event and f_{ol} is of the bigger event. In other words, the smaller event is the numerator and the bigger the denominator. The low frequency asymptote of *F(f)* is given by $g = \Omega_{ol}^{os}$ and the high frequency one $h = \Omega_{ol}^{os}(f_{os}/f_{ol})^2$, namely, the ratio of the acceleration flat level. Figure 2 (b) shows the observed spectral ratios with thin curves and their average over the available stations with a thick curve. To this thick curve the theoretical *F(f)* is fitted using a heuristic search; a combination of Down Hill Simplex Method with Very Fast Simulated Annealing (DHSM-VFSA; Press et al., 2002; Ingber 1989; Yokoi 2005). Figure 2 (c) shows this averaged curve and the best-fitting curve of *F(f)*. The high frequency asymptote *h* of the averaged curve can be seen clearly in Figure 2(c), whereas the low frequency one *g* cannot be seen due to growing of the curve from around 0.4Hz toward the lower frequency side.

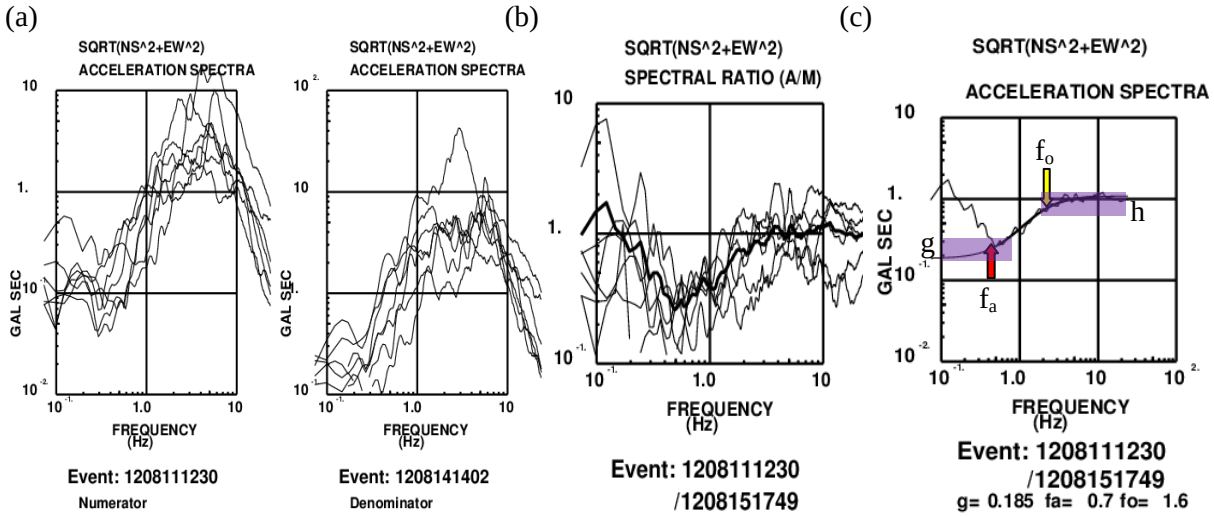

Figure 2. Example of analysis. (a) Acceleration spectra of the smaller event (Numerator: Event 1208111230) and the bigger event (Denominator: Event 1208151749) obtained at various stations. (b) Spectral ratio at various stations (thin curves) and their average over stations (thick curve). (c) Best fitting curve to the average spectral ratio curve, red arrow shows the determined corner frequency of the big event (f_a).

3. RESULT AND DISCUSSION

The spectral inversion was conducted using the above mentioned three divisor sites and two reference events. Due to the sparsity of available records, it was necessary to eliminate same aftershocks that were recorded at only few stations and same stations that obtained records during only few earthquakes. The final results were obtained using 13 stations and 35 earthquakes, among them three divisor sites and two reference events. Figure 3 shows the result of analysis for $Q^{-1}(f)$. In general, the spectral inversion method implicitly assumes that the radiation coefficient is the average value over azimuth and take-off angle. It is widely known that this assumption works well for the frequency range higher than around 5Hz; that the radiation coefficient follows the theory at the frequency range lower than around 1.0Hz; and that it has a transient behavior between them (e.g., Liu and Helmberger, 1985; Takemura et al., 2009). If various events are recorded at various stations evenly distributed, an averaging effect can be expected in the inversion process. However, in this study the records were sparsely obtained and each used pairs has only few spectral ratio curves. Therefore, it is expected that the method itself can fail in the low frequency range. The inverted $Q^{-1}(f)$ in Figure 3(b) (blue curve) shows the different trend below and above 2.3Hz. Considering the above mentioned condition, I selected the frequency range for the regression analysis above it (black curve). Fitting by the regression analysis was conducted on $log(f)$ - $log(Q^{-1})$ plot as shown in Figure 3(a). The result is,

$$Q(f) = 45.85 \times f^{1.495}, \quad (10)$$

where 45.85 is the value for Q_0.

Figure 4 shows the site effects for 13 stations inverted simultaneously. Damirchi (DMC002) has only one peak at around 7 Hz that reaches to 12 times of amplification. Khajeh (KJH007) has only one peak at around 3Hz that reaches to 10 times of amplification. Others show more complicated feature.

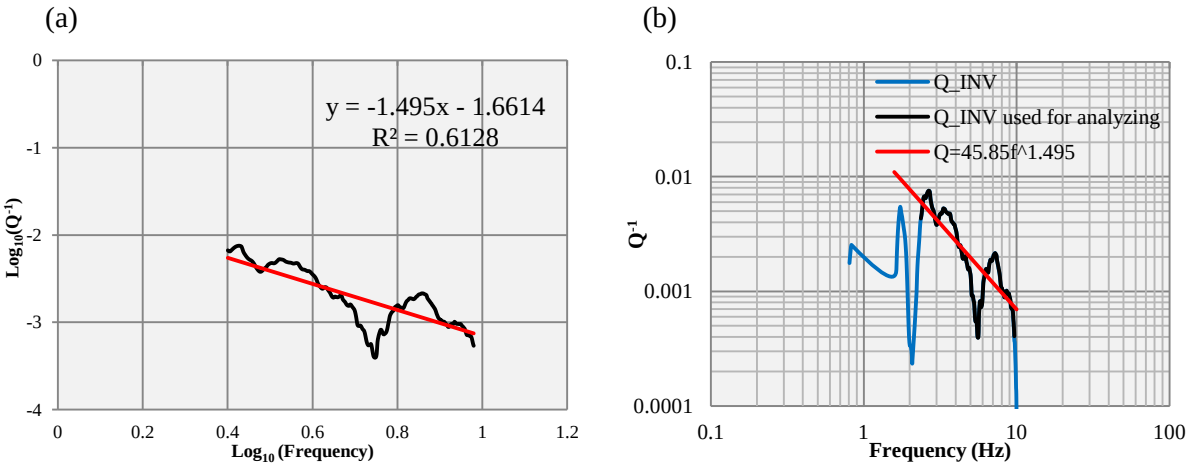

Figure 3. (a) Relation of inverted $Q^{-1}(f)$ against log(f) to find linear regression line; (b) Comparison of fitting: blue curve shows the inverted $Q^{-1}(f)$; black curve the data range used for regression analysis in the panel (a); red line the regression curve.

Meshgin Shahr (MES010), Kharvanagh (KHV006), Sheykh-Khomloo (SHK012) and Ahar (AHR001) have similar shape of amplification but different amplification, i.e., a lower peak at around 7 Hz and broad peaks from 1.5 Hz to 4 Hz. Only SHK012 has the highest peak at 1.5Hz. Hoorand (HUR004) has the site effect reaches to 10 times in the frequency range from 5 Hz to 7 Hz with minor ones at lower frequency. Peak at around 7 Hz appears at Chaykandi (CHK018) also but with peaks of similar height at 3.5 Hz and 1.5 Hz. Ahar (AHR001), Varzaqan (VAZ009) and Nahand (NHN008) show the site effect of which peaks are less than 5.0. Mehtarloo (MHL013), Haris (HAS003) and Kaleibar (KAL005) have a peak slightly bigger than 5.0. These 6 stations can be categorized as relatively low amplification sites. Nahand (NHN008) is the lowest. In contrast, Meshgin Shahr (MES010), Kharvanagh (KHV006), Damirchi (DMC002), Hoorand (HUR004) and Chaykandi (CHK018) are the group of relatively high amplification sites. By comparison between these stations the effects of sedimentary medium, including Lahar which is also rock formation such as conglomerates and breccia, on site effect become clear. Hence, more information from these types of ground materials is needed. Moreover, ground and underground identification with regard to topography, crash zones and fragmented regions is essential. Therefore, for these especial regions, in order to understand the geological structure responsible for these site effects more field activity including geotechnical data, seismic engineering and geological engineering data will be needed (Herrin et al., 2002).

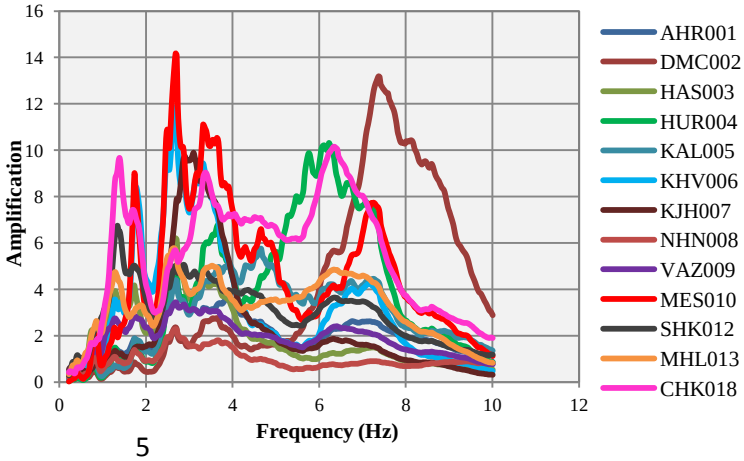

Figure 4. Site effects obtained from 13 stations using 35 events.

4. CONCLUSION

75 stations and 35 events were selected for analyzing, however, for stable solution, finally by using 13 stations and 35 events were used. In order to get even better result 3 divisor sites were introduced, i.e., Varzaghan (VAZ009), Horand (HUR004) and Mehtarloo (MHL013). Finally, two reference events were selected, 1208111223 as the first mainshock with magnitude 6.2 and 1211070626 as the aftershock with magnitude 5.3. By using these data, *Q-factor* was obtained which was $45.85\ f^{1.495}$. The site effect shows significant amplification in Meshgin Shahr (MES010), Kharvanagh (KHV006), Damirchi (DMC002), Hoorand (HUR004), Khajeh (KJH009) and Chaykandi (CHK018). The advantage of the spectral inversion method using the reference events is that in case of lack of data especially that of the reference site or when the reference site does not record enough data, reliable result including site effect and *Q-factor* can be obtained. Although the reference sites are not necessary, the usage of the reference events, especially the determination of the source parameters, can be quiet tough. It may be better to use a rock site or to conduct the geophysical exploration in sites where not so deep sediment is expected.

ACKNOWLEDGEMENTS

I would like to send my gratitude to Dr. Noorbakhsh MIRZAEI, head of Iranian Seismological Center (IRSC) and all staff members from the Institute of Geophysics University of Tehran (IGUT). Waveforms data obtained by Building and Housing Research Center (BHRC) Iranian National Broadband Seismic Network belongs to International Institute of Engineering Earthquake and Seismology (INSN-IIEES). Geological data used in this study belongs to Geological Survey of Iran (GSI).

REFERENCES

Andrews, D. J., 1986, American geophysical union, Washington, 67-259.
Boore, D. M. and Boatwright, J., 1984, Bull. Seism. Soc. Am., Vol. 74, pp.1615-1621.
Herrin E. T., Negraru T. P., Golden, P. and Mulcahy, C., 2002, No. DTRA01-00-C-0093 24th Seismic Research Review, 940-949.
Husid, P., 1967, California institute of technology Pasadena, California, 1-153.
Ingber, L., 1989, Mathematical and Computer Modeling, 12, 967–973.
Iwata, T. and Irikura, K., 1988, J. Phys. Earth 36, 155-184.
Liu, H. L. and Helmberger D. V., 1985, Bull. Seism. Soc. Am., vol. 75 no. 3, 689-708.
Moya, A. and Irikura, K., 2003, Bull. Seism. Soc. Am., Vol. 93, 1730-1745.
Press, W. H., Teukolsky A., Vetterling W. T. and Flannery B. P., 2002, Cambridge University Press.
Takemura, S., Furumura, T. and Saito T., 2009, Geophys. J. Int., Vol. 178, 950–961.
Web page: http://www.bhrc.ac.ir/portal/.
Web Page: http://www.iiees.ac.ir/.
Web page: http://geophysics.ut.ac.ir/Fa /.
Web page: http://earthquake.usgs.gov/earthquakes/eqarchives/poster/2012/20120811.php/.
Yokoi, T., 2005, Seismological Society of Japan Fall Meeting, Program and Abstract B049.